

SAXS by nanostructured materials.

Basic aspects and applications

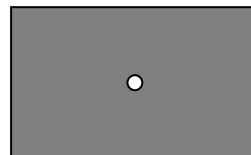
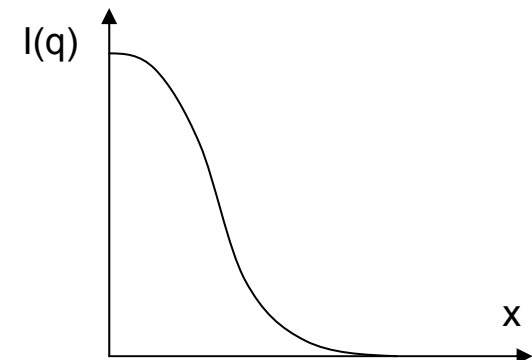
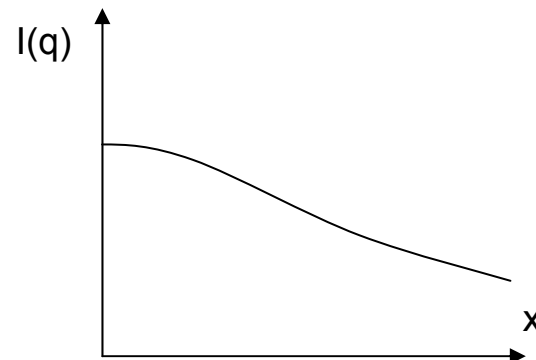
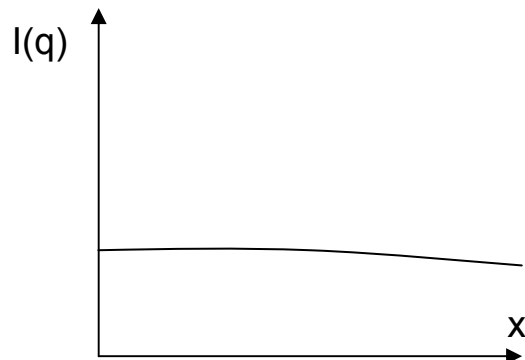
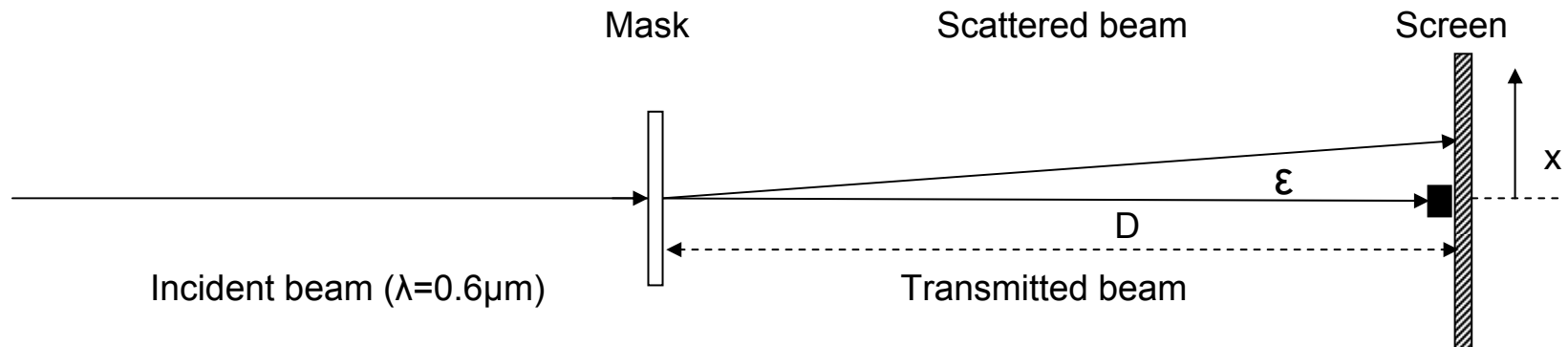
Aldo F. Craievich
Institute of Physics
University of São Paulo
São Paulo – SP Brasil

craievich@if.usp.br

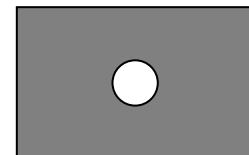
Content

- First Part: Basic theory and experimental setups
- Second Part: Applications

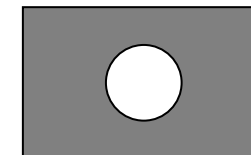
Schematic introduction



$R_1 \approx 1\mu\text{m}$

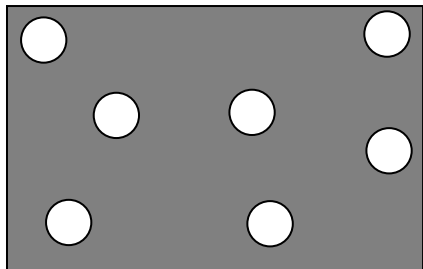


$R_2 \approx 5\mu\text{m}$

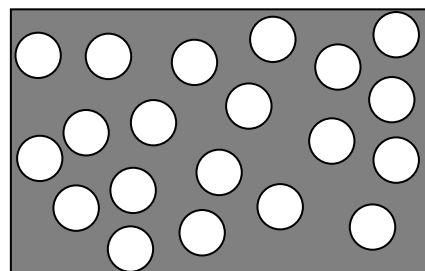


$R_3 \approx 20\mu\text{m}$

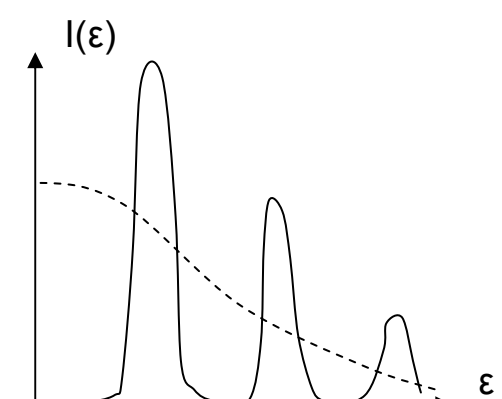
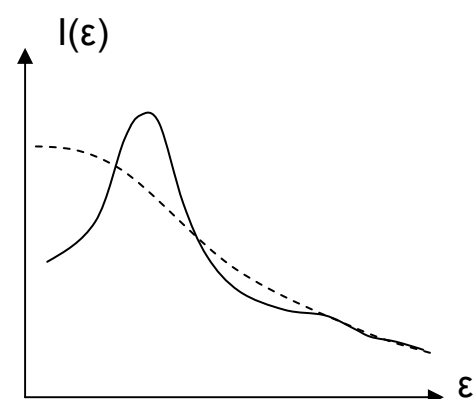
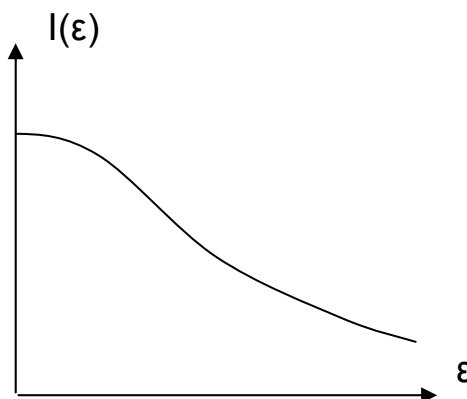
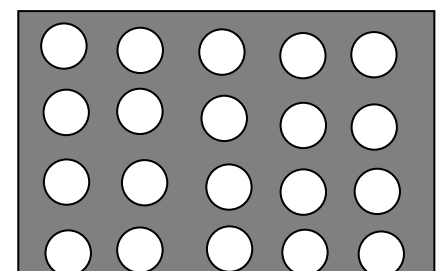
“Gas”



“Liquid”



“Solid”



Scattering of x-rays by an electron

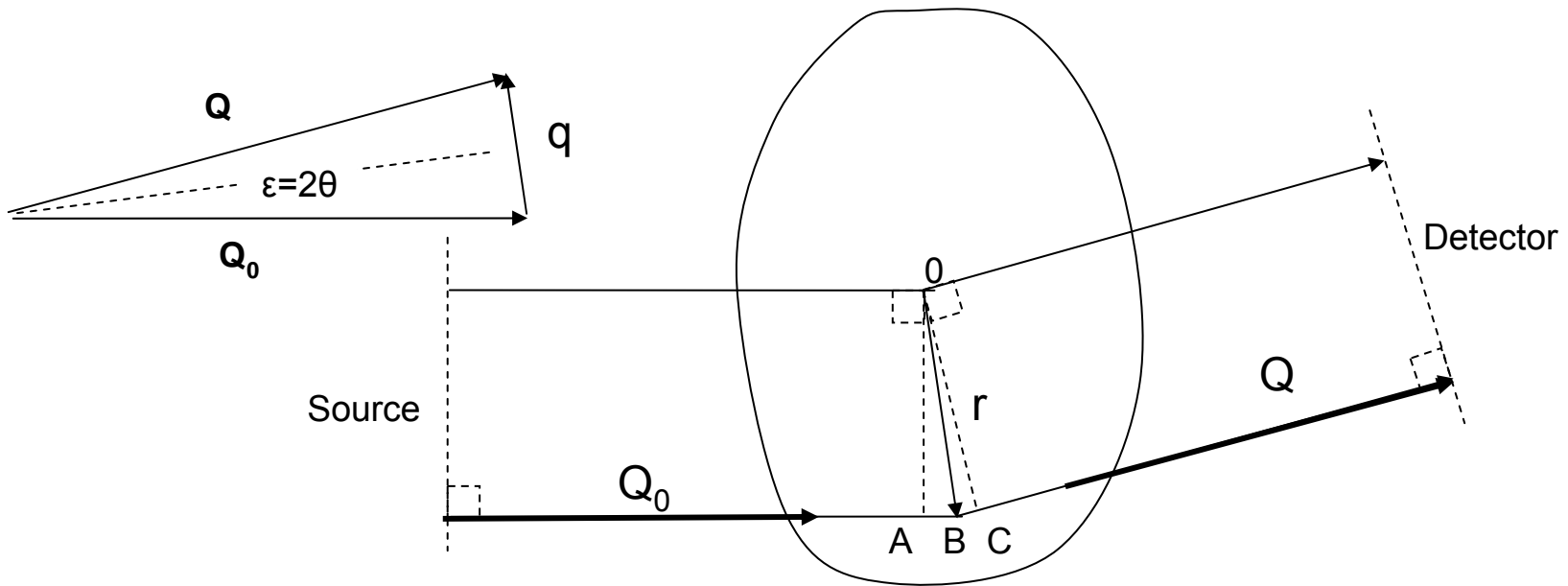
$$I_e(2\theta) = I_0 r_e^2 \left(\frac{1 + \cos^2 2\theta}{2} \right)$$

$$I_e(2\theta) = I_0 r_e^2$$

Basic equations

$$\Delta s = AB + BC = -(\hat{Q}_0 \cdot \vec{r} - \hat{Q} \cdot \vec{r})$$

$$\Delta\varphi = -2\pi \frac{(\hat{Q} - \hat{Q}_0) \cdot \vec{r}}{\lambda} = -(\vec{Q} - \vec{Q}_0) = -\vec{q} \cdot \vec{r}$$



$$\frac{A(\vec{q})}{A_e} = \int_V \rho(\vec{r}) e^{-i\vec{q} \cdot \vec{r}} d\vec{r} \quad \rho(\vec{r}) = \int \left[\frac{A(\vec{q})}{A_e} \right] e^{i\vec{q} \cdot \vec{r}} d\vec{q}$$

$$\gamma(\vec{r}) = \frac{1}{I_e} \int I(\vec{q}).e^{i\vec{q}.\vec{r}} d\vec{q} \quad |A(q)| = [I(q)]^{1/2}$$

$$\rho(\vec{r})=\rho_0+\Delta\rho(\vec{r})$$

$$\frac{A(\vec{q})}{A_e} = \int_V \rho_0 e^{-i\vec{q}.\vec{r}} d\vec{r} + \int_V \Delta\rho(r) e^{-i\vec{q}.\vec{r}} d\vec{r} \quad \frac{A(\vec{q})}{A_e} = \int_V \Delta\rho(r) e^{-i\vec{q}.\vec{r}} d\vec{r}$$

$$I(\vec{q}) = I_e \iint_{V V} \Delta\rho(\vec{r}_1) \Delta\rho(\vec{r}_2) . e^{-iq.(\vec{r}_1 - \vec{r}_2)} . d\vec{r}_1 d\vec{r}_2$$

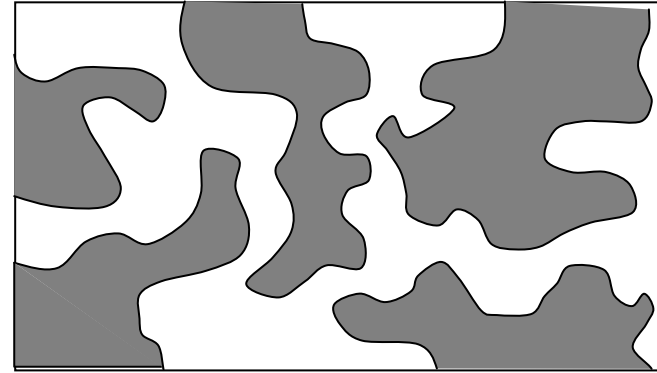
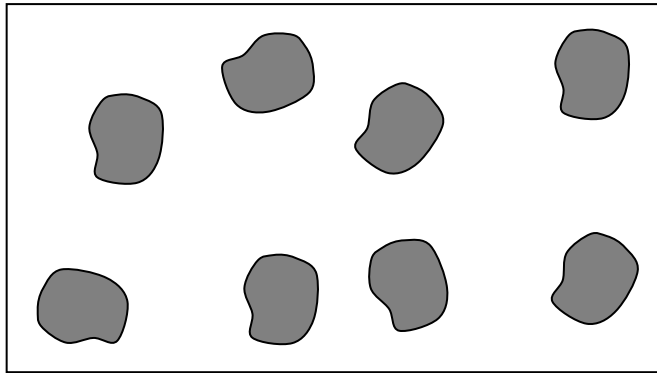
$$\vec{r}_1 - \vec{r}_2 = \vec{r}$$

$$I(\vec{q}) = I_e \iint_{V V} \Delta\rho(\vec{r}_2 + \vec{r}) \Delta\rho(\vec{r}_2) . e^{-i\vec{q}.\vec{r}} d\vec{r}_2 d\vec{r}$$

$$I(\vec{q}) = I_e V \int_V \gamma(\vec{r}) e^{-i\vec{q}.\vec{r}} d\vec{r}$$

$$\gamma(\vec{r}) = \frac{1}{V} \int_V \Delta\rho(\vec{r}') \Delta\rho(\vec{r}' + \vec{r}) . d\vec{r}' = \overline{\Delta\rho(\vec{r}') \Delta\rho(\vec{r}' + \vec{r})}$$

Small-angle scattering by a macroscopically isotropic material



$$\langle e^{-i\vec{q} \cdot \vec{r}} \rangle = \frac{\sin qr}{qr}$$

$$\gamma(r) = \frac{1}{8\pi^3 V I_e} \int_0^\infty 4\pi q^2 I(q) \frac{\sin q.r}{q.r} dq$$

$$\gamma(0) = \frac{1}{V} \int_V \Delta\rho(\vec{r}) \cdot \Delta\rho(\vec{r}) d\vec{r} = \overline{\Delta\rho(\vec{r})^2}$$

$$I(q) = I_e V \int_0^\infty 4\pi r^2 \gamma(r) \frac{\sin q.r}{q.r} dr$$

$$\gamma(0) = \frac{1}{8\pi^3 V I_e} Q$$

$$Q = \int_0^\infty 4\pi q^2 I(q) dq$$

Small-angle scattering by an arbitrary two electron density model

The reduced correlation function

The integral of the scattering intensity in reciprocal space

Asymptotic behavior of scattering curves at high q. Porod's equation

$$\gamma(r) = \varphi_1 \varphi_2 (\rho_1 - \rho_2)^2 \gamma_0(r) \quad I(q) = I_e V \varphi_1 \varphi_2 (\rho_1 - \rho_2)^2 \int_0^\infty 4\pi r^2 \gamma_0(r) \frac{\sin qr}{qr} dr$$

$$\gamma_0(r) = 1 - \frac{S/V}{4\varphi_1 \varphi_2} r + \dots \quad \gamma_0(r) = \frac{1}{8\pi^3 V I_e \varphi_1 \varphi_2 (\rho_1 - \rho_2)^2} \int_{Vq}^\infty 4\pi q^2 I(q) \frac{\sin qr}{qr} dq$$

$$Q = \int_0^\infty 4\pi q^2 I(q) dq$$

$$Q = 8\pi^3 V I_e \varphi_1 \varphi_2 (\rho_1 - \rho_2)^2$$

$$\gamma(r) = \varphi_1 \varphi_2 (\rho_1 - \rho_2)^2 \left(1 - \frac{S}{4V\varphi_1 \varphi_2} r \right) \quad I(q) = I_e V \varphi_1 \varphi_2 (\rho_1 - \rho_2)^2 \int_0^\infty 4\pi r^2 \left(1 - \frac{S \cdot r}{4V\varphi_1 \varphi_2} \right) \frac{\sin qr}{qr} dr$$

$$I(q) = \frac{2\pi I_e (\rho_1 - \rho_2)^2 \cdot S}{q^4}$$

Porod law

Small-angle scattering of a dilute system of isolated nano-objects.
General equations
The reduced correlation function for a single isolated object

$$I(q) = \sum_{i=1}^N I_1(\vec{q}) = N \left[\frac{1}{N} \sum_{i=1}^N I_1(\vec{q}) \right] \quad I(q) = N \langle I_1(\vec{q}) \rangle$$

$$\gamma_0(r) = 1 - (S_1 / 4V_1)r \quad \gamma_0(r) = \gamma(r) / [(V_1/V)(\rho_1 - \rho_2)^2]$$

$$\int_V 4\pi r^2 \gamma_0(r) dr = V_1$$

$$I_1(q) = I_e (\rho_1 - \rho_2)^2 V_1 \int_0^{D_{\max}} 4\pi r^2 \gamma_0(r) \frac{\sin q.r}{q.r} dr$$

$$I(0) = I_e N (\rho_1 - \rho_2)^2 V_1^2$$

$$V_1 = 8\pi^3 \frac{I(0)}{Q}$$

Asymptotic trend of the scattering intensity at small q. Guinier law

Dilute and monodispersed system (identical nano-objects)

$$I(q) = I_e N (\rho_1 - \rho_2)^2 V_1 \int_0^{D_{\max}} 4\pi r^2 \gamma_0(r) \frac{\sin qr}{qr} dr$$

$$I(q) = I_e N (\rho_1 - \rho_2)^2 V_1 \int_0^{D_{\max}} 4\pi r^2 \gamma_0(r) \left(1 - \frac{q^2 r^2}{6}\right) dr \quad (\sin qr / qr) = 1 - (q^2 r^2 / 6) + \dots$$

$$I(q) = I_e N (\rho_1 - \rho_2)^2 V_1^2 \left[1 - \frac{q^2}{6} \frac{1}{V_1} \int_0^{D_{\max}} 4\pi r^2 \gamma_0(r) dr \right] = I_e N (\rho_1 - \rho_2)^2 V_1^2 \left[1 - \frac{q^2}{6} R_g^2 \right]$$

$$R_g^2 = \frac{1}{V_1} \int_0^{D_{\max}} 4\pi r^2 \gamma_0(r) dr$$

$$R_g = \left\{ \frac{\int_V \rho(\vec{r}) \cdot r^2 d\vec{r}}{\int_V \rho(\vec{r}) d\vec{r}} \right\}^{1/2}$$

$$R_g = \left[\frac{1}{V} \int_V r^2 d\vec{r} \right]^{1/2} = \overline{r^2}$$

$$I(q) = I_e N (\rho_1 - \rho_2)^2 V_1^2 \cdot e^{-\frac{R_g^2 q^2}{3}}$$

$$R_g = \sqrt{3/5} R$$

$$R_g = \sqrt{(D^2 / 8) + (H^2) / 12}$$

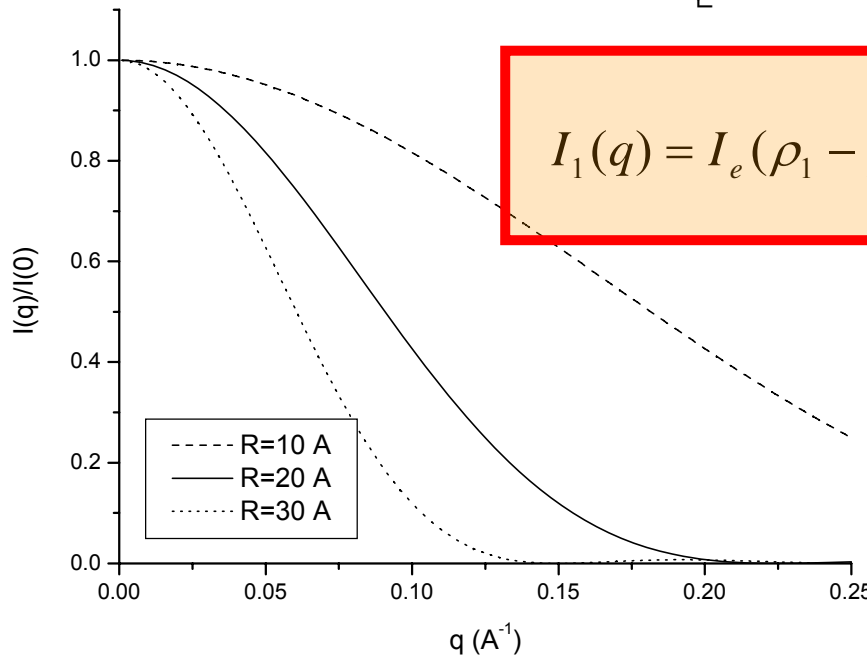
Spherical nano-objects embedded in a homogeneous matrix

$$I(q) = \int N(R).I_1(q, R)dR$$

$$\gamma_0(r) = 1 - \frac{3r}{R} + \frac{1}{16} \left(\frac{r}{R} \right)^3$$

$$I_1(q) = I_e (\rho_1 - \rho_2)^2 V_1 \int_0^R \left[1 - \frac{3r}{R} + \frac{1}{16} \left(\frac{r}{R} \right)^3 \right] 4\pi r^2 \frac{\sin qr}{qr} dr$$

$$I_1(q) = I_e (\rho_1 - \rho_2)^2 \left(\frac{4\pi R^3}{3} \right)^2 [\Phi(q)]^2$$

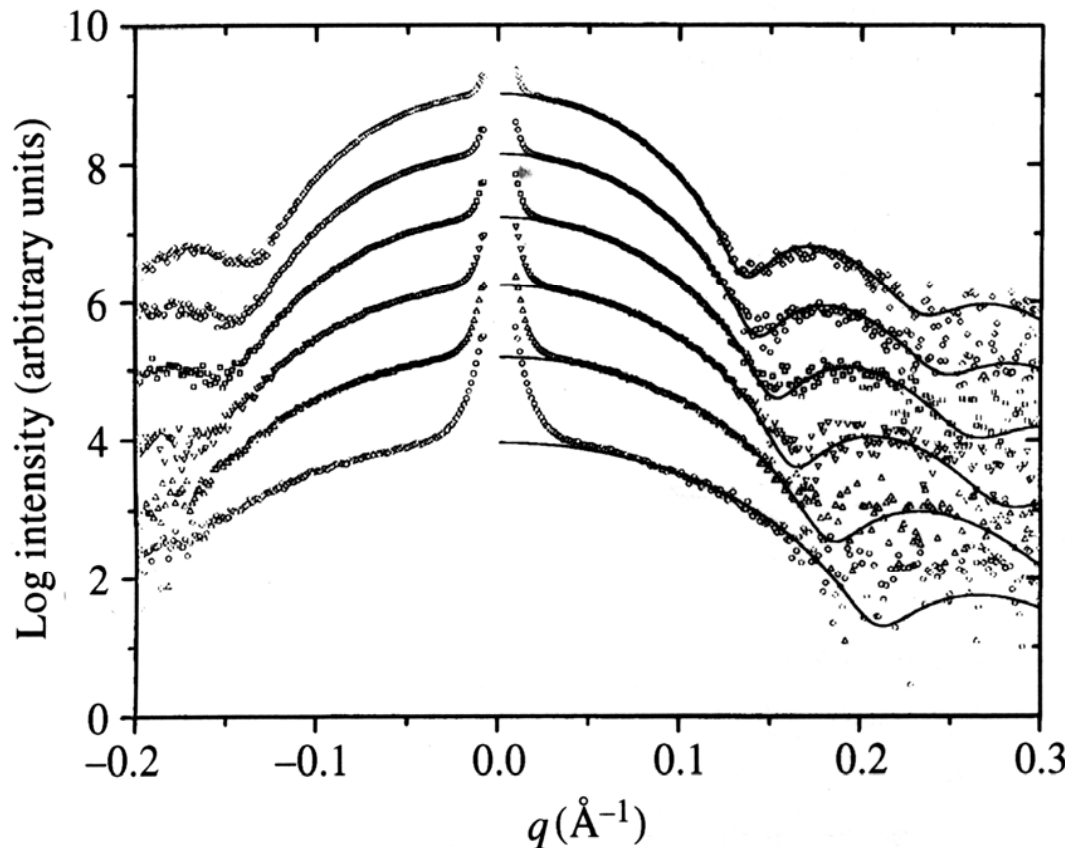


$$\Phi(q) = 3 \frac{\sin qR - qR \cos qR}{(qR)^3}$$

$$D(R) = \frac{4\pi}{3} R^3 . N(R)$$

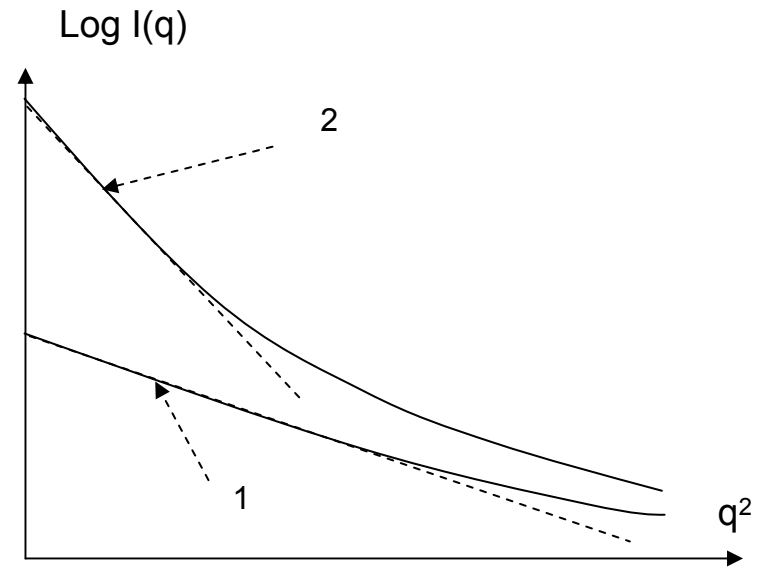
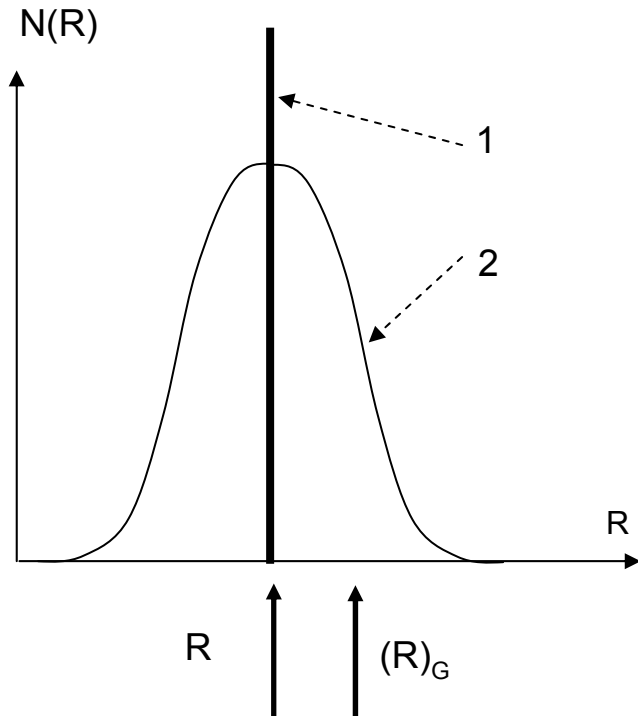
$$I(q) = I_e (\rho_1 - \rho_2)^2 \left(\frac{4\pi}{3} \right)^2 \int N(R) R^6 \left[3 \frac{\sin qR - qR \cos qR}{(qR)^3} \right]^2 dR$$

*PbTe nano-crystals embedded in a homogeneous silicate glass,
(Kellermann et al)*



Scattering intensity curves corresponding to a dilute set of spherical PbTe nano-crystals during isothermal growth ($T=650\text{C}$) [9]. The continuous line is the best fit of Eq. (66) using a Gaussian $N(R)$ function with a time varying radius average and a constant relative standard deviation $[\sigma / \langle R \rangle] = 0.08$. The curves were vertically displaced for clarity

Dilute and isotropic system of polydispersed nano-objects



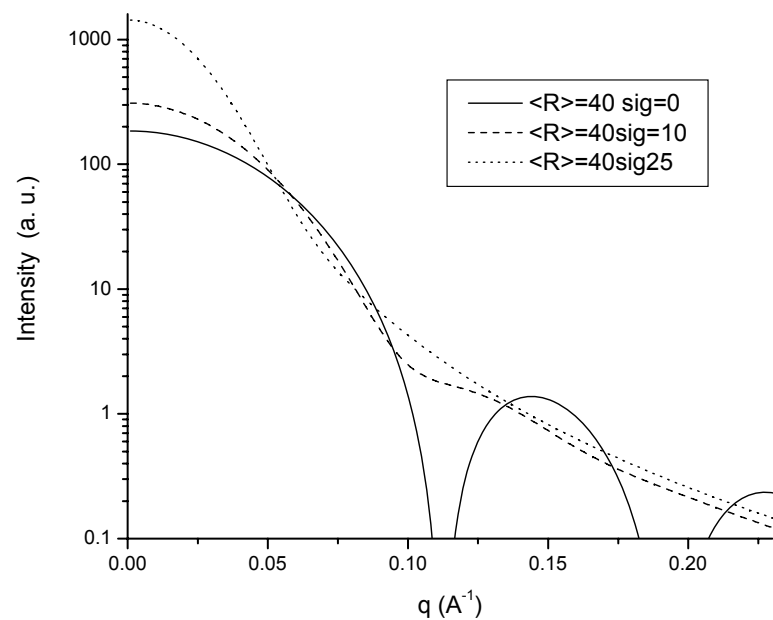
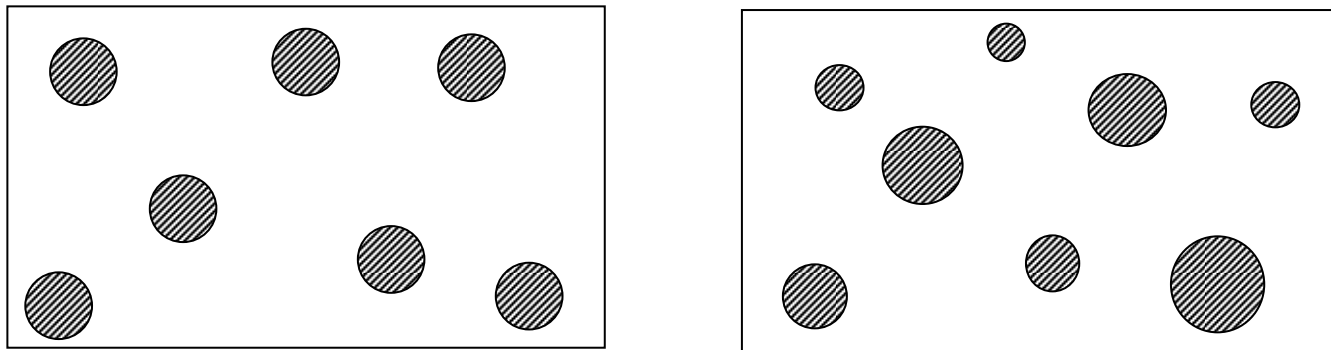
$$I(\vec{q}) = I_e (\rho_1 - \rho_2)^2 \int N(R_g) \cdot V_1^2(R_g) \cdot e^{-\frac{R_g^2 q^2}{3}} dR_g$$

$$I(q) = NI_e (\rho_1 - \rho_2)^2 \cdot \langle V_1^2 \rangle e^{-\frac{\langle R \rangle_G^2 q^2}{3}}$$

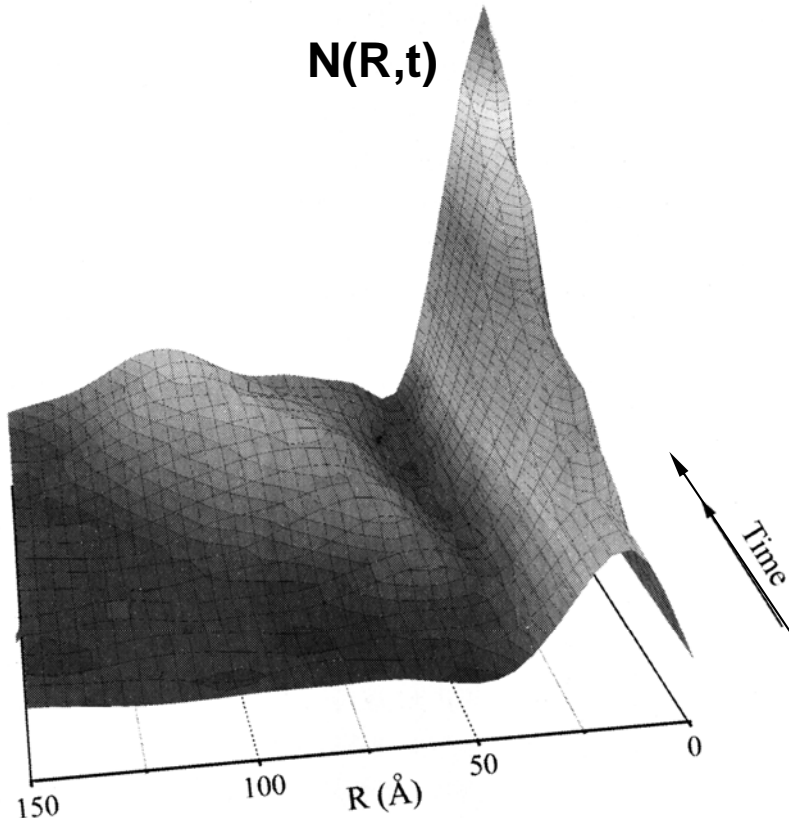
$$I(q) = NI_e (\rho_1 - \rho_2)^2 \left[\frac{1}{N} \int N(R_g) \cdot V_1^2(R_g) \cdot dR_g - \frac{q^2}{6N} \int N(R_g) \cdot V_1^2(R_g) \cdot R_g^2 dR_g \right]$$

$$\langle V_1^2 \rangle = \frac{1}{N} \int N(R_g) \cdot V_1^2(R_g) dR_g$$

$$\langle R \rangle_G = \left[\frac{1}{N} \int N(R_g) \cdot V_1^2 \cdot R_g^2 dR_g \right]^{1/2}$$



ZnO based colloidal suspensions (Tokumoto et al).



Time-dependent volume distribution functions $D(R)$ of ZnO colloidal particles maintained inside a sealed cell during SAXS measurements [14].

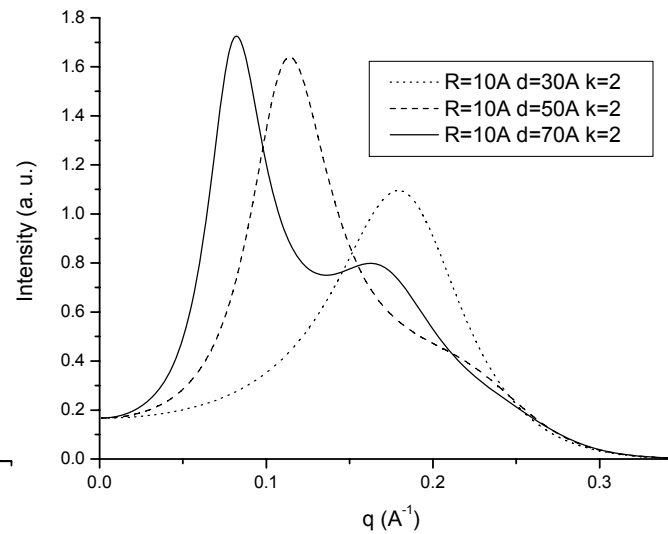
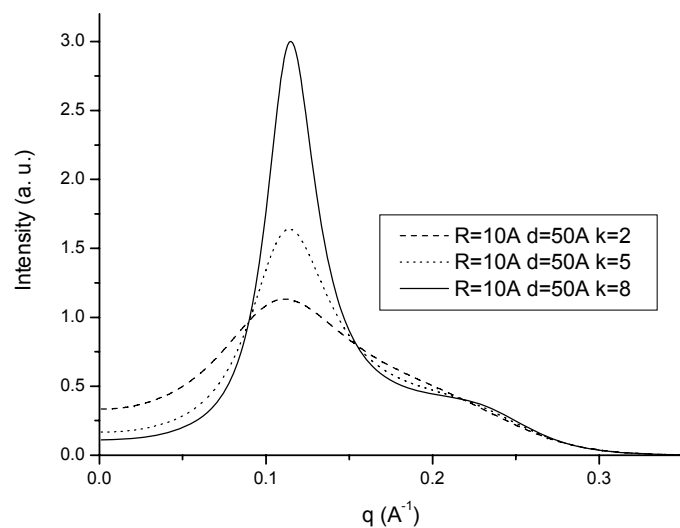
The time increases from 10 up to 120 min.

The volume functions were derived, using the GNOM package [10], from the set of experimental SAXS curves.

Spherical nano-objects embedded in a solid matrix

Dense systems

$$I(q) = N \cdot I_1(q) \cdot S(q)$$

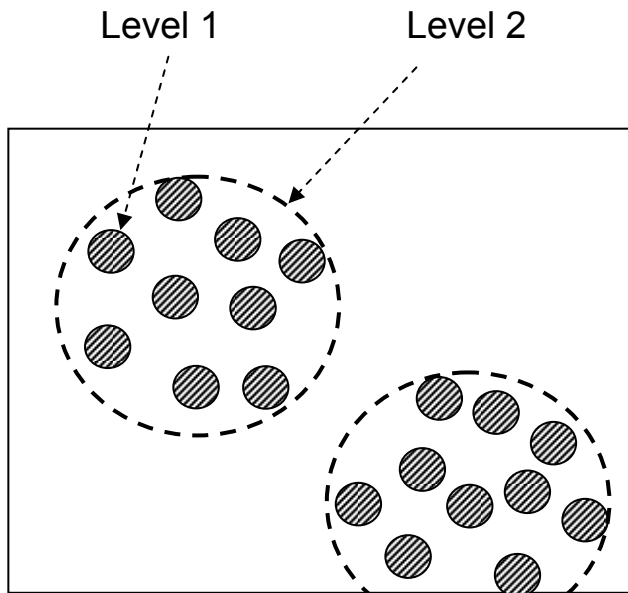


$$S(q) = \frac{1}{1 + k\Phi(qd)}$$

$$\Phi(qd) = 3 \frac{\sin(qd) - qd \cos(qd)}{(qd)^3}$$

$$d = \frac{2\pi}{q_{\max}}$$

(79)



Level 2

Level 1

Log I(q)

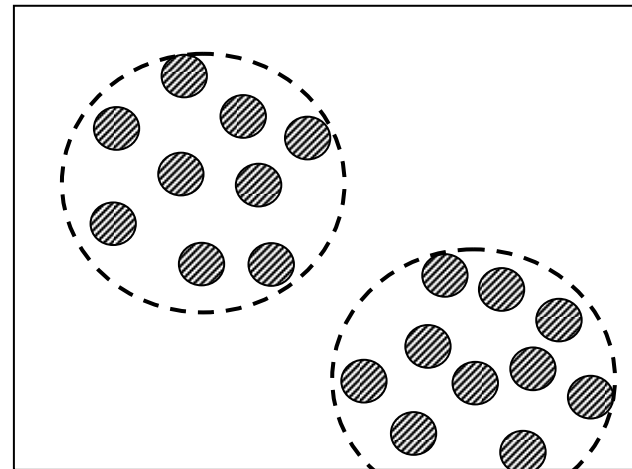
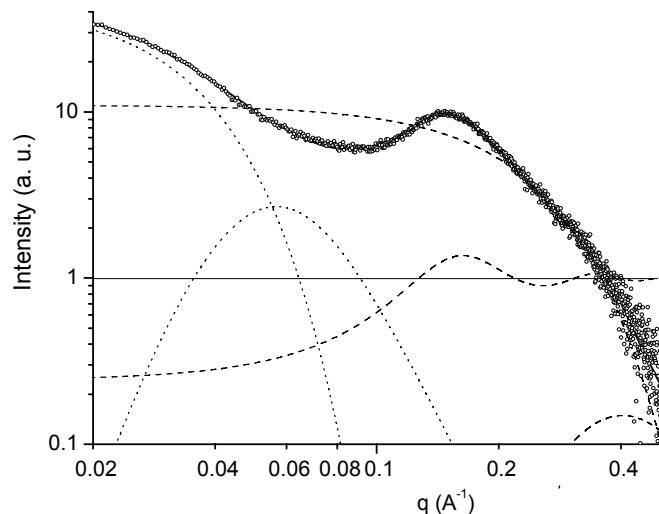
(80)

Log q

$$I(q) = \left[G_1 \cdot e^{-\frac{1}{3}R_{g1}^2q^2} + B_1 \cdot e^{-\frac{1}{3}R_c^2q^2} \left\{ \text{erf}\left(qR_{g1}/6^{1/2}\right) \right\}^3 / q \right]^4 + \left[G_2 \cdot e^{-\frac{1}{3}R_{g2}^2q^2} + B_2 \cdot \left\{ \text{erf}\left(qR_{g2}/6^{1/2}\right) \right\}^3 / q \right]^4$$

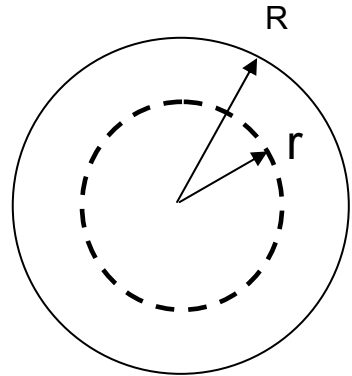
$$I(q) = \sum_{i=1}^n \left[G_i \cdot e^{-\frac{1}{3}R_{gi}^2q^2} + B_1 \cdot e^{-\frac{1}{3}R_{g(i+1)}^2q^2} \left\{ \text{erf}\left(qR_{gi}/6^{1/2}\right) \right\}^3 / q \right]^4$$

Fe(II) doped di-ureasil hybrids (Silva et al)

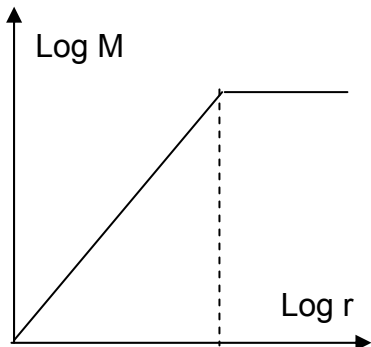


$$I(q) = S_1(q) \left[G_1 \cdot e^{-\frac{1}{3} R_{g1}^2 q^2} + B_1 \cdot e^{-\frac{1}{3} R_c^2 q^2} \left\{ \operatorname{erf} \left(q R_{g1} / 6^{1/2} \right) \right\}^3 / q \right] + \left[G_2 \cdot e^{-\frac{1}{3} R_{g2}^2 q^2} + B_2 \cdot \left\{ \operatorname{erf} \left(q R_{g2} / 6^{1/2} \right) \right\}^3 / q \right]$$

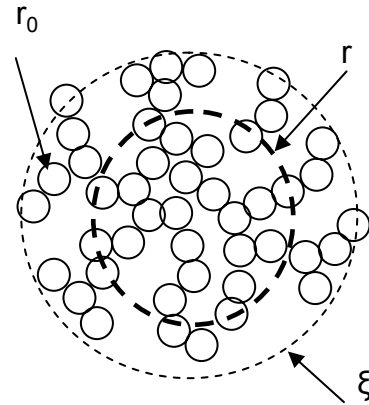
Experimental scattering intensity from a sample containing 0.76 weight % Fe(II). The continuous line is the best fit of Eq. 94 to the experimental curve. The dashed lines indicate the Guinier and Porod contributions to the scattering intensity produced by siliceous clusters and the structure function (oscillatory curve). The point lines are the Guinier and Porod contributions to the scattering intensity yielded by the coarse domains [22].



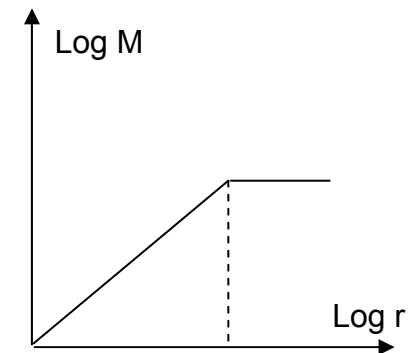
Homogeneous object



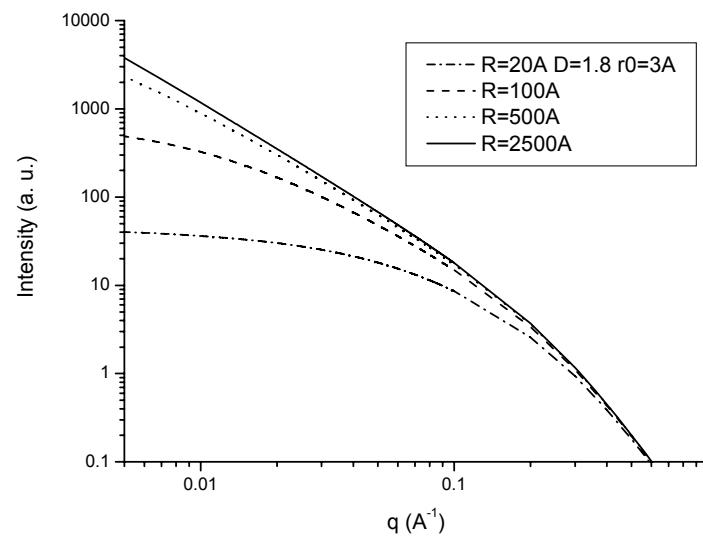
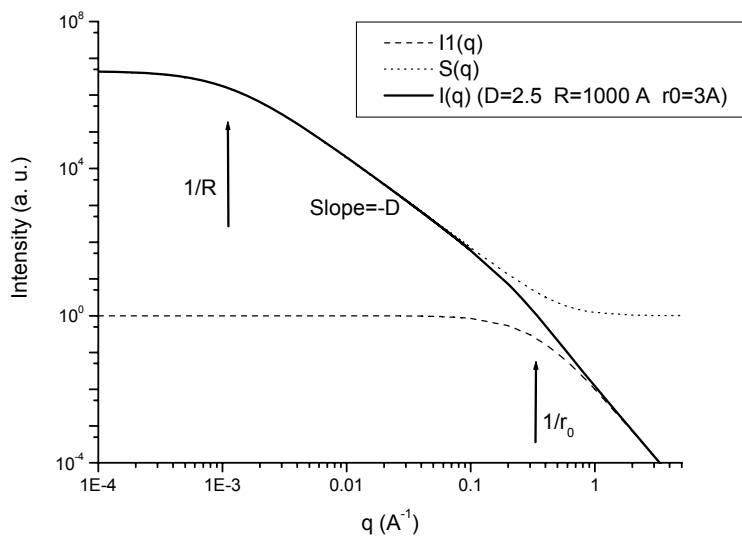
Slope 3



Fractal object



Slope D



$$N(r) \!=\! \left(\frac{r}{r_0}\right)^D \qquad \qquad \qquad \frac{N}{V} \, g(r) \!=\! \frac{N}{V} \!+\! \left(\frac{D}{4\pi r_0^D} \, r^{D-3} \right) e^{-r/\xi}$$

$$S(q)=1+\frac{D}{r_0^D}\!\int\limits_0^\infty\!r^{D-1}e^{-\frac{r}{\xi}}\,\frac{\sin qr}{qr}dr\qquad\qquad\qquad I(q)=\frac{A}{\left(1+r_0^2q^2\right)^2}$$

$$S(q)=1+\frac{1}{\left(qr_0\right)^D}\frac{D.\Gamma(D-1)}{\left[1+1/(q^2\xi^2\right]^{(D-1)/2}}\sin\!\left[(D-1)\tan^{-1}(q\xi)\right]$$

$$\boxed{I(q)=\frac{A}{\left(1+r_0^2q^2\right)^2}.\left\{1+\frac{1}{\left(qr_0\right)^D}\frac{D.\Gamma(D-1)}{\left[1+1/(q^2\xi^2\right]^{(D-1)/2}}\sin\!\left[(D-1)\tan^{-1}(q\xi)\right]\right\}}$$

$$I(0)=\Gamma(D+1).\left(\frac{\xi}{r_0}\right)^D$$

$$S(q)=S(0)\bigg\{1-\bigg[\frac{D(D+1)}{6}\bigg]\xi^2q^2\bigg\}\cong S(0).e^{-\frac{R_g^2q^2}{3}}\qquad\qquad R_g=\bigg[\frac{D(D+1)}{2}\bigg]^{1/2}\,\xi$$

$$1/\,\xi << q << 1/\,r_0 \qquad\qquad\qquad I(q) \propto q^{-D}$$

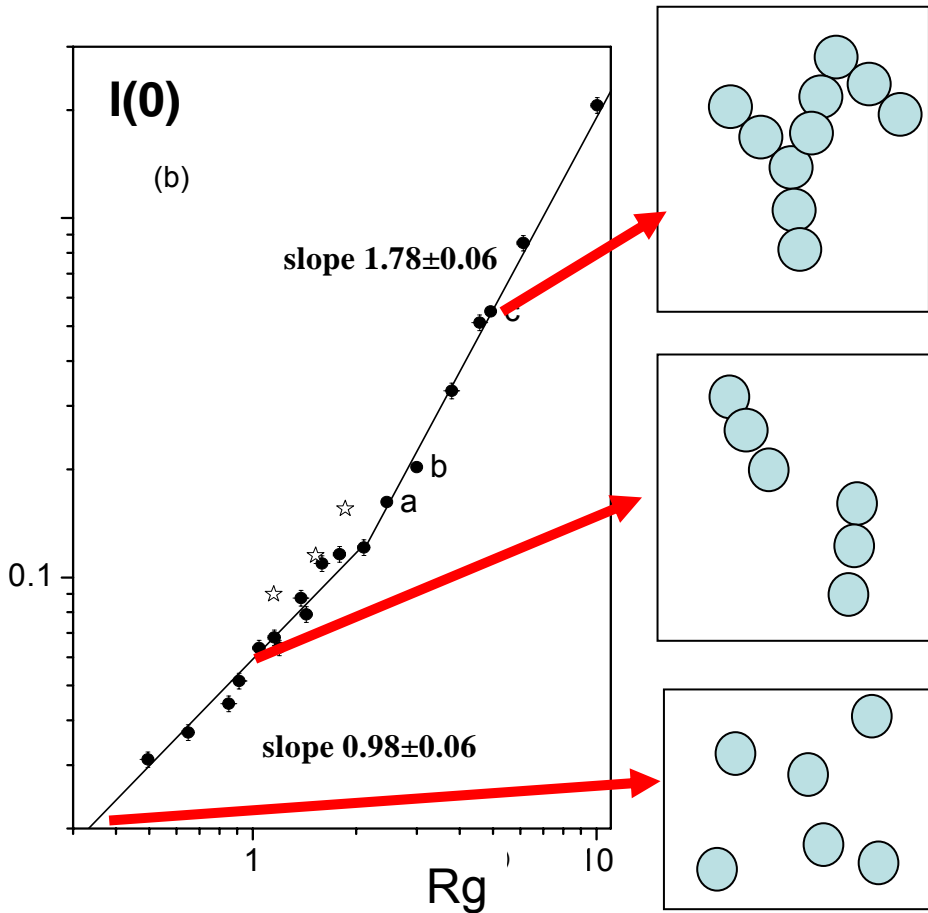
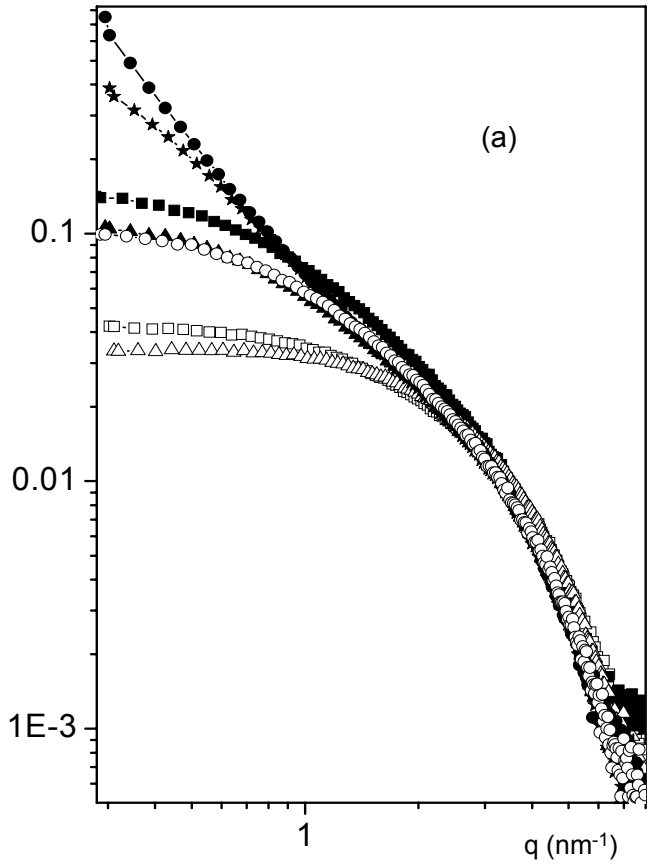
Aggregation of colloidal particles

Models of growth and results of calculations of the fractal dimension

using computer simulation

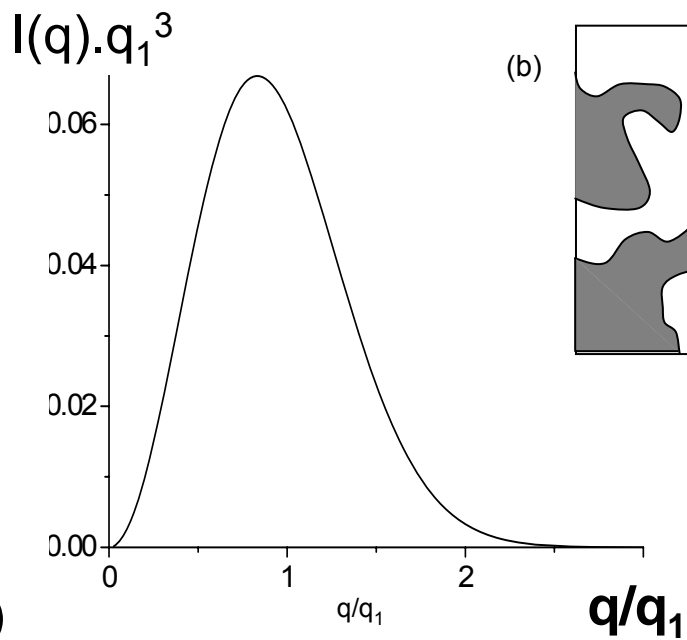
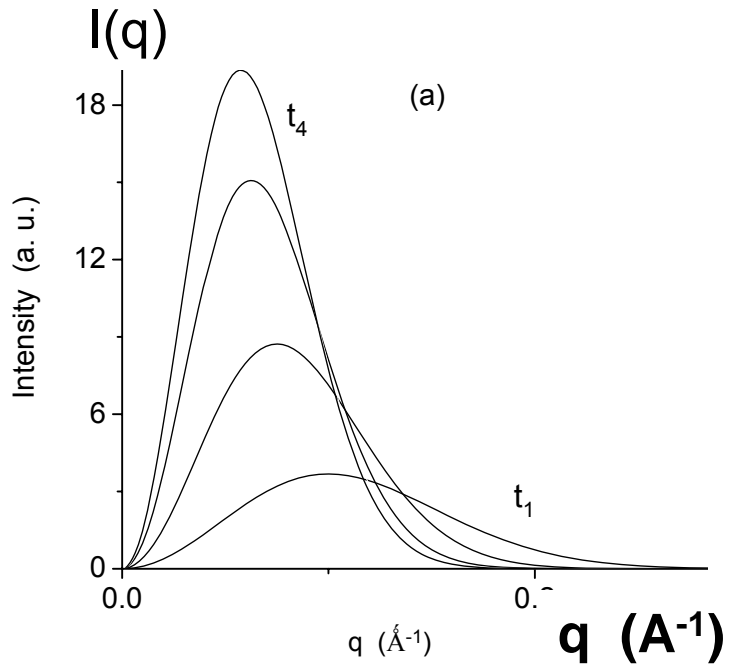
Mechanism of growth	Fractal dimension (3D)	Fractal dimension (2D)
Eden		2
Witten Sanders	2.45	1.65-1.70
Witten Sanders linear trajectory	2.97	1.92-1.95
Tip-to-tip	1.43	1.26
Self-avoiding walk	1.66	1.33
Cluster-cluster random walk	1.75-1.80	1.44-1.48
Cluster-cluster ballistic	1.81-1.95	1.50-1.54
Ideal linear polymer	2.00	
Swollen linear polymer	1.66	
Ideal branched polymer	2.16	
Dense particle	3.00	
Diffusion limited cluster-cluster aggregation (DLCA)	1.78	
Reaction limited cluster-cluster aggregation (RLCA)	2.11	

**Sulfate-zirconia sols with different HNO₃, H₂SO₄ and H₂O contents.
(Riello et al)**



Scattering intensity of a few selected samples inside a sealed cell in their final aggregation state. (b) Plot of $I(0)$ vs. R_g , in log-log scale, corresponding to the final states of sols with different H₂SO₄ contents [19].

Nanophase separation and dynamical scaling property.



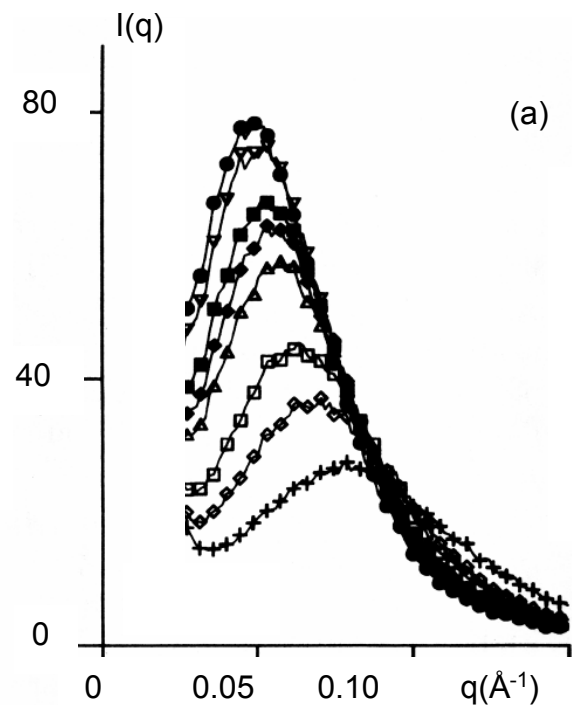
$$I(q, t) = N \cdot I_1(q) \cdot S(q \cdot t) \propto S(q, t)$$

$$q_n(t) = \left[\frac{\int_0^\infty q^n(t) \cdot I(q, t) dq}{\int_0^\infty I(q, t) dq} \right]^{1/n}$$

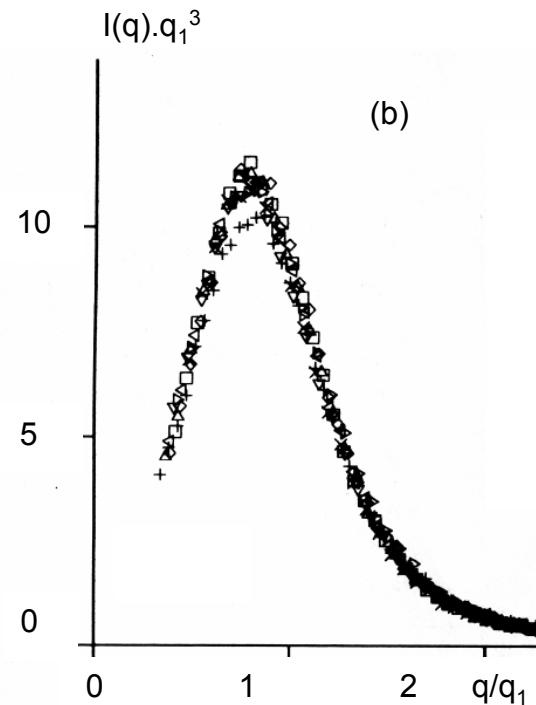
$$F(x) = I(q, t) \cdot [q_1(t)]^3$$

- a)** Different scattering intensity curves from a system in advanced stages of nanophase separation for increasing periods of isothermal annealing from t_1 to t_4 .
(b) Scaled structure function,

SnO_2 based porous xerogels (Santilli et al)



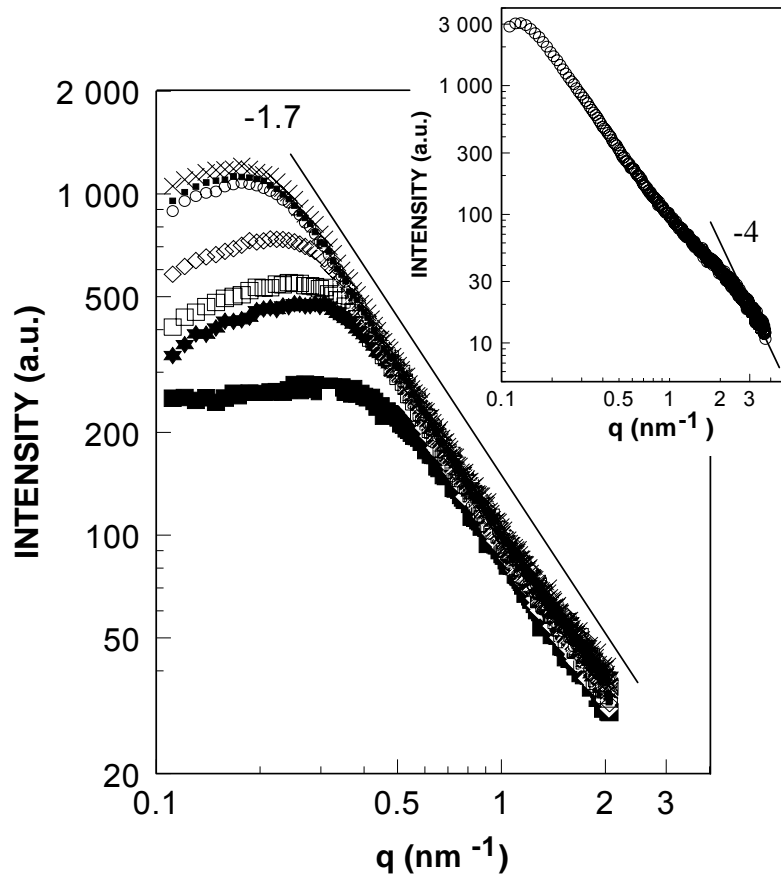
(a)



(b)

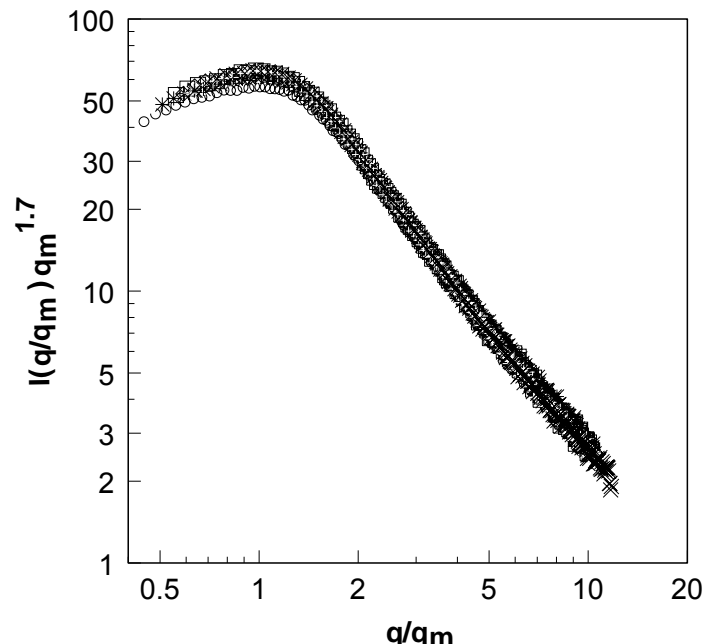
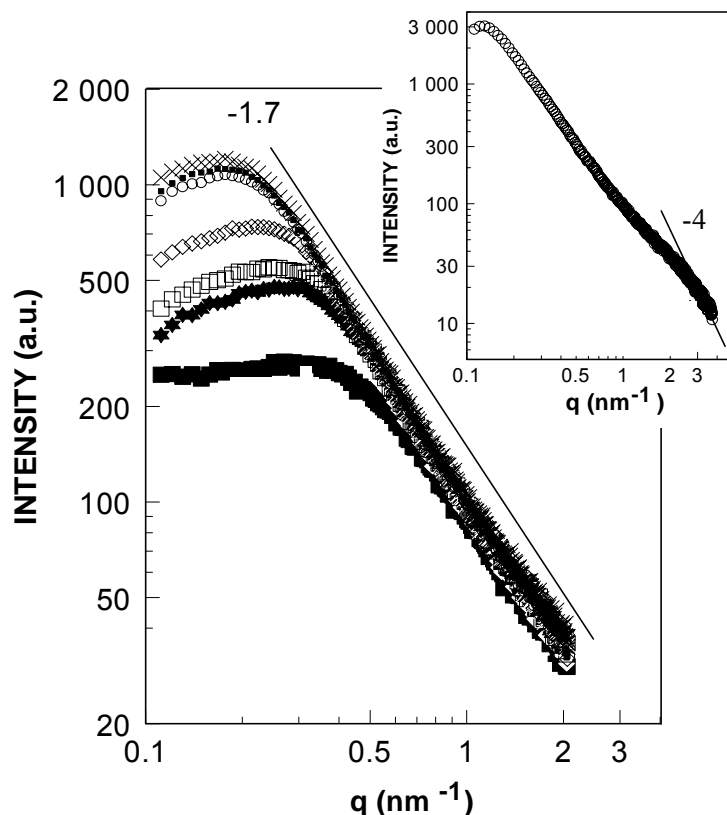
a) Scattering intensity curves correspondin to a nanoporous SnO_2 xerogel held at 400C during increasing periods of time frrom 4.5 min. (bottom) up to 62.5 min (top) [27].
b) Same curves plotted as $[I(q,t)q_1^3]$ versus (q/q_1) .

Zirconia-based sols (Lecomte et al)



Log I vs. log q plots for increasing periods of time from 4 hours (bottom) up to 742 hours (top) [21]. The inset is the scattering intensity curve of the final gel

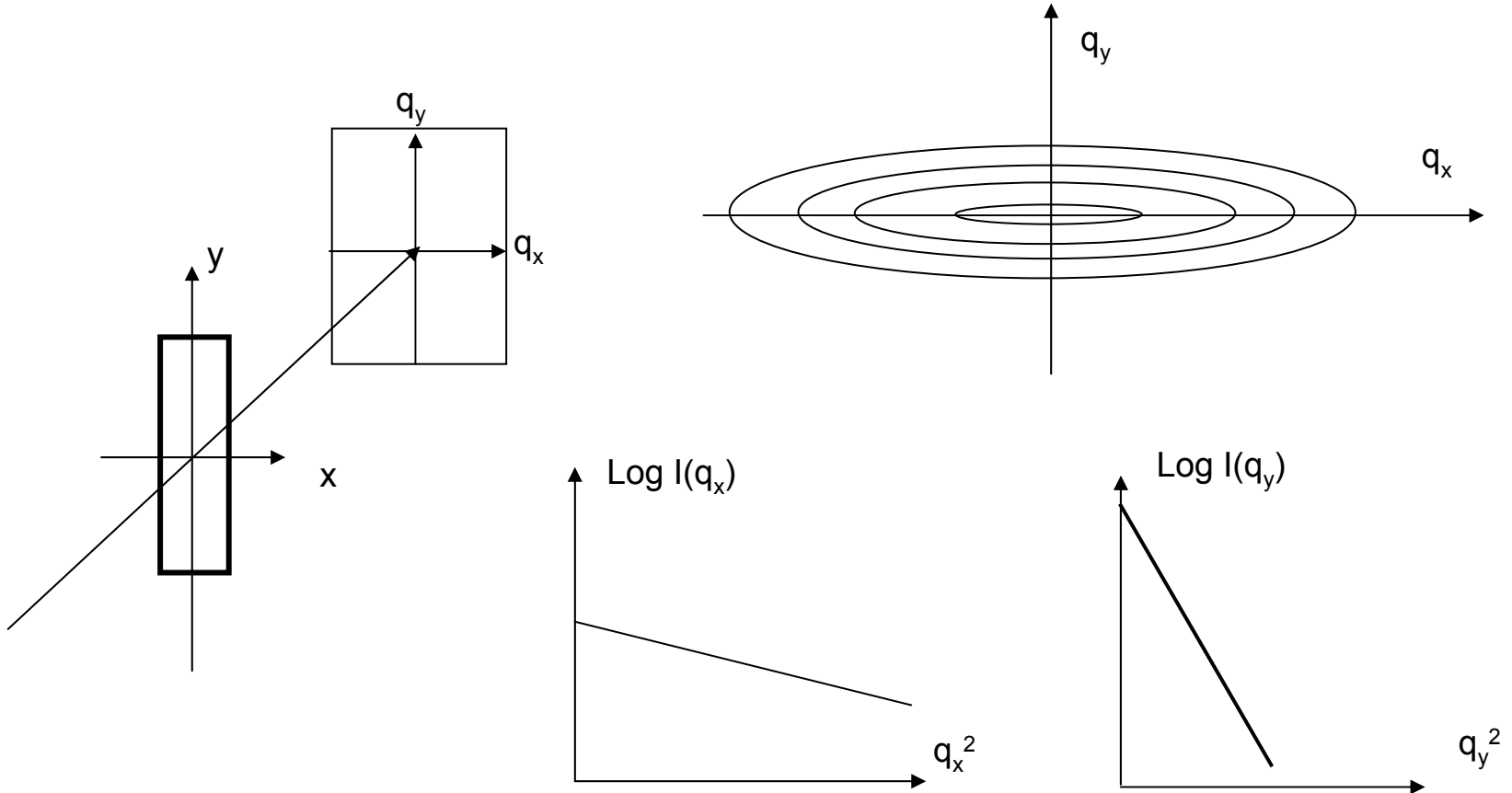
Zirconia-based sols (Lecomte et al)



Scattering intensity curves replotted as

$[I(q)q_m^{1.7}]$ versus (q/q_m) [21],

q_m being the q value corresponding to the maximum of the scattering curves (Assumption $q_m \sim q_1$).



$$I_1(q_D) = N(\rho_1 - \rho_2)^2 V_1^2 e^{-R_D^2 \cdot q_D^2}$$

$$R_D = \frac{1}{V} \int_V r_D^2 \cdot d\vec{r} = \overline{r_D^2}$$

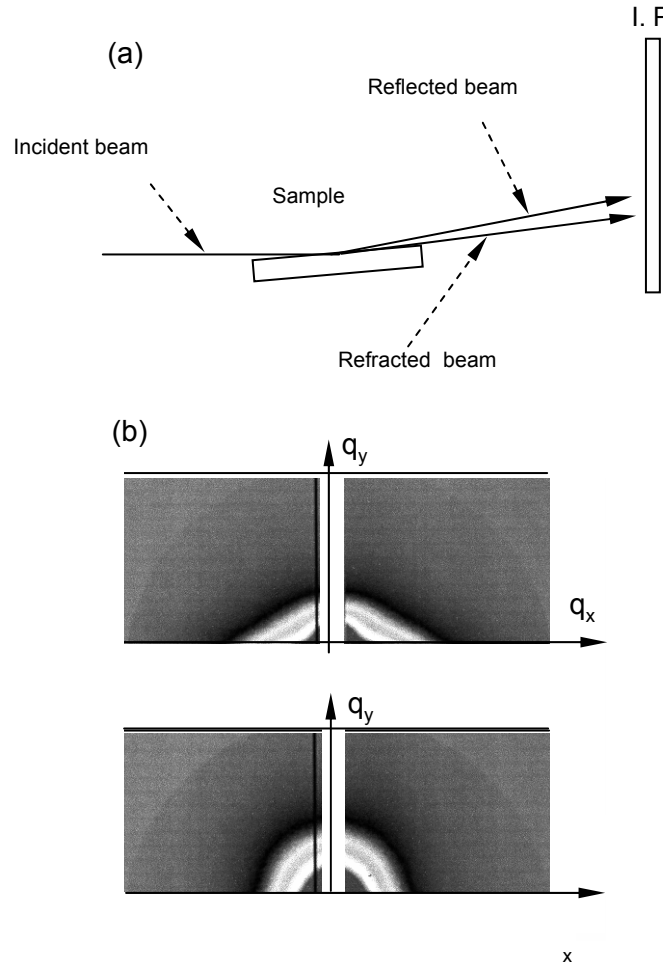
4.3.2. Dilute and isotropic system of very anisotropic nano-objects

$$qI(q) \propto e^{-\frac{1}{2} R_c^2 q^2}$$

$$q^2 I(q) \propto e^{-R_t^2 q^2}$$

$$R_t = T / \sqrt{12}$$

Zn-based thin films prepared by dip coating (Tokumoto et al).



(a) Schematic GISAXS setup.

**(b) GISAXS patterns recorded with an image plate
for In-doped ZnO-based films prepared by the pyrosol procedure [29].
Top: Film deposited on a glass substrate at 350C.
Bottom: Film deposited on a glass substrate at 450C.**